

# $T_c$ map and superconductivity of simple metals at high pressure

Wei Fan, Y. L. Li, J. L. Wang, L. J. Zou and Z. Zeng

Key Laboratory of Materials Physics,  
Institute of Solid State Physics, Hefei Institutes of Physical Sciences,  
Chinese Academy of Sciences, 230031-Hefei, People's Republic of China

August 18, 2010

## Abstract

We calculate  $T_c$  map in region of weak electron-phonon coupling based on simple phonon spectrum. By using linear-response method and density functional theory, we calculate phonon spectra and Eliashberg functions of simple metals under pressure. Based on the evolutions of superconducting parameters of simple metals on the  $T_c$  map with increasing pressure, we find that there are two different responses to pressure for simple metals: (1) enhancing electron-phonon interaction  $\lambda$  such as for La and Li, (2) increasing phonon frequency such as for Pb, Pt. The  $\lambda$  threshold effect is found, which origins from the competition between electron-phonon interaction and electron-electron Coulomb interaction and is the reason why  $T_c$  of most superconductors of simple metals are higher than 0.1K.

Key Words:  $T_c$  Map, superconductivity, pressure, simple metals

PACS: 74.62.Fj, 74.20.Fg, 74.25.Dw

## 1 Introduction

The BCS theory and its strong-coupling generalization (Eliashberg theory) have successfully explained the superconductivity of elementary metals and their alloys [1, 2]. In strong electron-phonon coupling region  $\lambda \gg \mu^*$ , Eliashberg equation has been widely studied, where  $\lambda$  is the parameter of electron-phonon interaction and  $\mu^*$  is Coulomb pseudo-potential. However in weak-coupling region  $\lambda$  is comparable with  $\mu^*$ . The competitions between electron-phonon interaction and electron-electron interaction are so prominent that some new aspects of Eliashberg equation can be found in such region. The Eliashberg equation is very hard to be solved using analytic method. In fact no analytic solution has been found except for some extreme limit. The numerical methods can overcome the difficulties encountered by analytic method and provide full and global information on Eliashberg equation. The  $T_c$  maps in three-dimensional parameter space  $\Omega - \lambda - \mu^*$  had been calculated [3], which can predict the possible highest transition temperature for a certain superconducting material and light the route to find superconductors with higher  $T_c$  [3]. It's very interesting to

study the evolution of superconducting parameters on the  $T_c$  map with external parameter such as pressure.

The issues on the superconductivity of simple elements become active due to the developments of high pressure technique based on diamond-anvil cell (DAC). The  $T_c$  of metal lithium can reach about 20K at high pressure [4, 5]. The researches along this direction have been extended to non-metal elements, such as sulphur [6], oxygen [7] and diamond [8], non-magnetic metals such as non-magnetic iron [9], calcium [10] and yttrium [11]. Some of them have very complex lattice structures, rich structural phase diagrams and corresponding structural phase transitions. Thus from structural complexity point of view, these simple elements, such as lithium and boron, are not really simple. The  $T_c$  of these superconductors generally change with the changes of crystal structures. At very high pressure some simple metals even transform to insulator phase or semiconductor phase [12, 13]. An introduction for the superconductivity of simple elements can be found in a short review [14].

Theoretically, the linear response method in the framework of density functional theory has been widely used to calculate the superconducting properties of simple elements [15, 16]. These calculations reproduce very well the transition temperatures of some elements such as metal lithium [17, 18], yttrium [19] and lanthanum [20, 21] at high pressure. In this paper we present the information on so-called  $T_c$  map [3] in weak-coupling region. The numerical calculations in weak-coupling region are more difficult than those in strong-coupling region because the very low  $T_c$  needs more Matsubara frequencies to obtain more numerically reliable  $T_c$ . In this work, we find the threshold effect of  $\lambda$ , which can explain why noble metals are not superconductors even at very high pressure. We use density functional theory and perturbed line-response theory to calculate the Eliashberg function  $\alpha^2 F(\omega)$ . We mainly concentrate on the non-magnetic simple metals and try to find how their  $T_c$  run on the  $T_c$  map with increasing pressure. With increasing pressure, two different pressure effects are found: (1) enhancing  $\lambda$  such as for La and Li and (2) increasing phonon frequency such as for Pb and Pt. The metals belong to the first group generally undergo complex structural phase transitions with increasing pressure.

## 2 Strong-Coupling theory

The energy-gap equation of Eliashberg-Nambu theory in the Matsubara's imaginary-energy form is standard and well established [1]. Firstly, we use a simple analytic model of Eliashberg function written in the form

$$\alpha^2 F(\omega) = \begin{cases} \frac{c}{(\omega - \Omega_P)^2 + (\Omega_2)^2} - \frac{c}{(\Omega_3)^2 + (\Omega_2)^2}, & |\omega - \Omega_P| < \Omega_3 \\ 0 & \text{others,} \end{cases} \quad (1)$$

where  $\Omega_P$  is the energy (or frequency) of phonon mode,  $\Omega_2$  the half-width of peak of phonon mode and  $\Omega_3 = 2\Omega_2$ . The parameter of electron-phonon interaction can be written as  $\lambda = \lambda(0) = 2 \int_0^\infty d\omega \alpha^2 F(\omega) / \omega$ . The moments  $\langle \omega^n \rangle$  of the distribution function  $(2/\lambda) \alpha^2 F(\omega) / \omega$  are defined as  $\langle \omega^n \rangle = 2/\lambda \int_0^\infty d\omega \alpha^2 F(\omega) \omega^{n-1}$ . Based on these moments, others frequency parameters are defined as  $\langle \omega \rangle_n = (\langle \omega^n \rangle)^{1/n}$ . Another important parameter is  $\langle \omega \rangle_{ln} = \exp[2/\lambda \int (d\omega/\omega) \alpha^2 F(\omega) \ln \omega]$ . The Coulomb pseudo-potential is defined as  $\mu_0 = N(0)U$  and its renormalized value is  $\mu^* = \mu_0 / (1 + \mu_0 \ln(E_C/\omega_0))$ , where  $U$  is the Coulomb parameter,  $N(0)$

the density of states at Fermi energy,  $E_C$  the characteristic energy for electrons such as the Fermi energy or band width, and  $\omega_0$  the characteristic phonon energy such as the energy cutoff of phonon energy or Debye energy. In the region of small  $\lambda$ , where  $T_c$  is generally smaller than 10K. To accurately define  $T_c$ , the number  $N$  of Matsubara energy must be larger enough to guarantee the range of energy larger than the maximum of phonon energy. We choose  $N=1000$ , the values of  $T_c > 0.1\text{K}$  are numerically reliable if  $\Omega_P < 60\text{ meV}$ .

There are two important  $T_c$  formulas based on strong coupling theory, which are the McMillan formula[2]

$$T_c = \frac{\langle\omega\rangle_1}{1.20} \exp\left[-\frac{1.04(1+\lambda)}{\lambda - \mu^*(1 + 0.62\lambda)}\right] \quad (2)$$

and the formula generalized by Allen [1]

$$T_c = \frac{f_1 f_2 \langle\omega\rangle_{ln}}{1.20} \exp\left[-\frac{1.04(1+\lambda)}{\lambda - \mu^*(1 + 0.62\lambda)}\right], \quad (3)$$

where  $f_1$  and  $f_2$  are the functions of  $\lambda$ ,  $\mu^*$ ,  $\langle\omega\rangle_2$  and  $\langle\omega\rangle_{ln}$ , which can be found in Ref.[1].

### 3 Threshold effect of $\lambda$

The McMillan's formula presents a threshold  $\lambda_a = \mu^*/(1 - 0.62\mu^*) > \mu^*$ . If  $\lambda < \lambda_a$ , the superconductivity will be destroyed by Coulomb interaction. A solution of Eliashberg equation had been found long time ago by Wu and his co-workers [22, 23, 24]. The formula is expressed as  $T_c = \alpha_{00} \sqrt{\lambda \langle\omega^2\rangle} S(1/\lambda)$ , where  $S(1/\lambda) = \sum_{j=0}^{\infty} b_j / \lambda^j$ . The formula is accurate in strong-coupling region. If number of Matsubara energies used in calculation is large enough the formula is analytic when  $\infty > \lambda > \lambda_a$  even with  $\lambda_a < 1.0$ . It had been proved that if  $N \gg 1$ ,  $\lambda_a \sim \mu^*$  [23]. When  $\lambda < \lambda_a$ , the  $T_c$  formula is not analytic and physically, superconductivity does exist. If the number  $N$  of Matsubara energies is large, the form of the  $T_c$  formula will be very complicated.

What is the threshold in general Eliashberg theory?. In this section we present our numerical solution by using large number of Matsubara energies up to  $N=5500$ . From Fig.1(a), we find that, for  $\lambda < 0.3$ , the results of strong-coupling calculations are considerably different from McMillan's and Allen's formulae. The strong-coupling theory used in this work shows a disrupted change for  $T_c$ . When  $\lambda < \lambda_c \sim 0.22 - 0.26$ , there are no superconductivity. The  $\lambda_c$  is dependent on the number of Matsubara energies. In our calculations, we increase the number from 200 to  $N=5500$ , the  $\lambda_c$  decreases from 0.26 to 0.22 with  $\mu^* = 0.1$ . If we use larger  $\mu^*$ ,  $\lambda_c$  also takes larger values. In Fig.1(b), we decrease  $\mu^*$  to zero, the  $\lambda_c$  decreases to about 0.10-0.11. The  $\lambda_c$  in many aspects are similar to  $\lambda_a$  obtained from McMillan formula, for instance,  $\lambda_c$  slightly larger than  $\mu^*$ . This means that  $\lambda_c = \mu^* + \delta\lambda$  and  $\delta\lambda > 0$ . If  $\mu^*=0$ ,  $\delta\lambda = 0.1 \sim 0.11$  shown in Fig.1(b).

The accurate  $\lambda_c$  is hard to define numerically because a very large  $N$  is needed to obtain reliable results if  $T_c < 0.0001\text{K}$ . This brings difficulties to define  $T_c$  if  $T_c < 10^{-4}\text{K}$  using numerical calculations of Eliashberg theory. At this time, McMillan formula is a good choice as shown in Fig.1(a,b). In the case of  $\mu^*=0.0$ ,

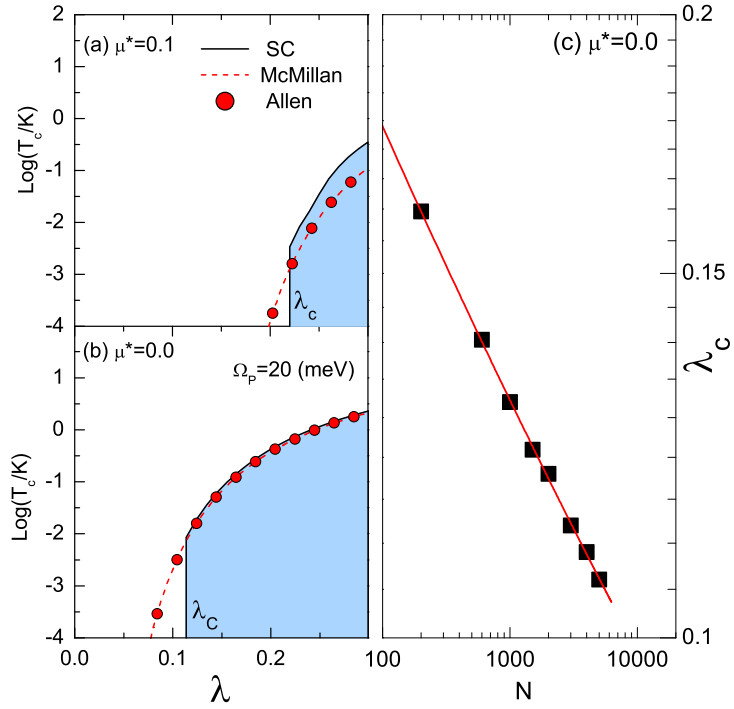


Figure 1: The comparison of strong-coupling theory with the McMillan's formula and the Allen's  $T_c$  formula. Two values of Coulomb pseudo-potential (a)  $\mu^*=0.1$  and (b)  $0.0$  are chosen but the energy of phonon  $\Omega_P=20$  meV keeps unchanged. The figure shows the jump of  $T_c$  when  $\lambda$  is smaller a certain threshold value  $\lambda_c$  which is about  $0.22$  when  $\mu^*=0.1$ . The (c) shows the  $N$ -dependent  $\lambda_c$  plotted with logarithm-scale axes.

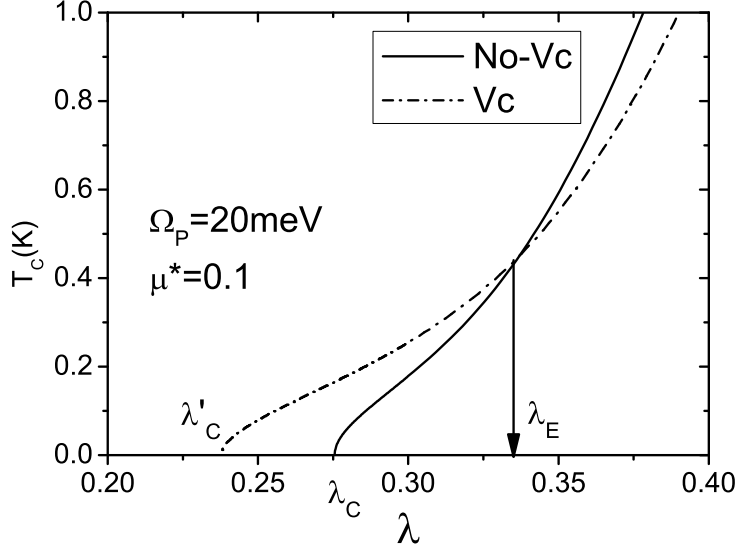


Figure 2: The effects of vertex corrections on  $\lambda_c$  using the same parameters as the Fig.1(a). The arrow shows the transition from negative vertex correction to positive vertex correction. The band-width parameter  $E_B=1$  eV is used in calculations.

the Fig.1(c) show  $N$ -dependent  $\lambda_c$  with logarithm-scale. we fit  $N$ -dependent  $\lambda_c$  using formula  $\lambda_c = AN^{-P} + \lambda_c^0$ . The fitting results are  $P=-0.16$  and  $\lambda_c^0=0.0299$ . This means that, if  $N \rightarrow \infty$ ,  $\lambda_c \rightarrow \lambda_c^0=0.0299$ . Thus our results imply that the threshold of  $\lambda$  exists, but not so large as shown in Fig.1. Additionally, there are many physical reasons that make  $\lambda_c$  not too small. In fact, only finite  $N$  is enough because of the existence of the cutoff for phonon energy (Debye energy). Moreover some pair-breaking interactions such as the interaction with magnetic order and magnetic fluctuation make  $\lambda_c$  larger.

We further study the influence of vertex correction or non-adiabatic effects on  $\lambda_c$ . Generally, we expect that in strong-coupling region with  $\lambda > 2$ , the vertex correction has significant influence on  $T_c$ . However in weak-coupling region from Fig.2, we find that the vertex correction can reduce  $\lambda_c$  to smaller value. This is closely related to the positive vertex correction  $T_c^V > T_c$  ( $T_c^V$  is transition temperature including vertex correction) that had been found in previous work [3]. The magnitude of vertex correction is dependent on the effective band-width, in which the smaller band-width is corresponding to the strong vertex correction. In Fig.2, the effective band-width is about 1.0 eV. The band widths of simple metals are generally larger than 1.0 eV so that the vertex correction has smaller effects than that shown in Fig.2.

We have found that both larger  $N$  and vertex correction make  $\lambda_c$  decrease to the small value. As an approximation, we define an approximate threshold  $\lambda_c=0.22-0.28$  if  $\mu^*=0.1$ . The region with  $\lambda < \lambda_c$  and  $T_c < 0.1K$  is called weak-superconductivity region. The superconductivity in this region is easily destroyed by pair-breaking interaction coming from magnetism or inhomogeneity of superconducting materials. In fact, for most of simple metals,  $T_c$  are

Table 1: Table.(1) The table provides the parameters of lattice constant  $a, b, c$  ( $\text{\AA}$ ),  $\lambda$  electron-phonon interaction,  $\langle\omega^2\rangle\lambda$  ( $\text{meV}$ )<sup>2</sup>, transition temperature  $T_c$  (K) calculated in this work and the experimental  $T_c^{exp}(K)$ . The numbers in parentheses behind  $T_c$  and  $T_c^{exp}$  are pressure. For the purpose of comparison the parameters  $\lambda$  obtained in other works are also provided. The second column is lattice parameters.

		$\lambda$		$\langle\omega^2\rangle\lambda$	$T_c$	$T_c^{exp}$
Ni	$a=3.51$	0.15		101	-	-
Pd	$a=3.97$	0.20	0.350 <sup>c</sup>	58.55	-	3.20 <sup>a</sup>
Pt	$a=4.00$	0.32		53.2	0.15	0.02 <sup>b</sup>
Cu	$a=3.62$	0.17	0.140 <sup>c</sup>	50.12	-	-
Ag	$a=4.15$	0.12	0.146 <sup>e</sup>	23.70	-	-
Au	$a=4.13$	0.21	0.170 <sup>d</sup>	19.16	-	-
Cd	$a=2.97$	0.55	0.710 <sup>e</sup>	31.8	0.98	0.52
	$c/a=1.88$					
Hg <sup>h</sup>	$a(b,c)=3.18$	1.85		21.1	4.87	4.15
	$\alpha(\beta, \gamma) = 70.52^\circ$					
Pb	$a=4.77$	1.41	1.680 <sup>c</sup>	50.0	8.01	7.20
Li <sup>f</sup>	$a=3.38$	0.33		202.2	22(41)	20(50)
Cs	$a=6.13$	0.12		0.95	-	1.66(8)
La <sup>g</sup>	$a=5.34$	0.986		63.24	6.84	6
Al	$a=3.95$	0.37	0.440 <sup>c</sup>	352.2	1.20	1.18
Tl	$a=3.45$	1.58		25.4	5.20	2.40
	$c/a=1.59$					

<sup>a</sup> Stritzker et al., irradiation with He<sup>+</sup> Ref.[28]; <sup>b</sup> Schindler et al., powder samples, Ref.[29]; <sup>c</sup> Savrasov et al., Ref.[15]; <sup>d</sup> Bauer et al., Ref.[30]; <sup>e</sup> Bose, Ref.[16] with  $\lambda$  of 3d and 4d transition metal elements; <sup>f</sup> fcc structure. At ambient pressure Li is metal with bcc structure without superconductivity. <sup>g</sup> fcc structure. <sup>h</sup> Rhombohedral structure.

larger than 0.1K except for W, Be, Pt and Rh.

$T_c$  changing discontinuously with  $\lambda$  will have significant effects on the superconductivity. Simple metals have very low  $T_c$  and their parameters of electron-phonon interaction  $\lambda$  are generally smaller than 0.5. The threshold effect can predict why some noble metals such as Au, Ag and Cu are not superconductors even under very-high pressure. The threshold effect determines why  $T_c$  of most of simple metals are higher than 0.1K. We will extend the Fig.1 to  $T_c$  map on  $\langle\omega\rangle_2 - \lambda$  plane (Fig.4) in the section 5.

## 4 The phonon spectrum and electronic-phonon interaction from the calculations of linear response method

With development of the method of electronic-structure calculation in solid materials, the Eliashberg function  $\alpha^2F(\omega)$  and the parameters of electron-phonon

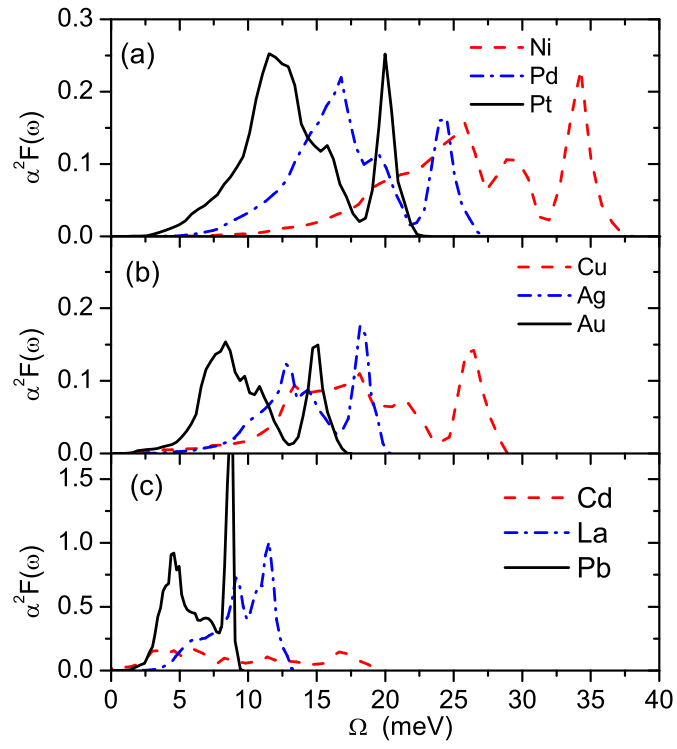


Figure 3: The Eliashberg-McMillan functions  $\alpha^2 F(\omega)$  for simple elements of Ni, Pd, Pt, Cu, Ag, Au, Cd, La and Pb.

interaction can be calculated using density functional theory combined with linear-response theory [15]. The  $q$ -dependent parameter of electron-phonon interaction is defined as

$$\lambda_{q\nu} = \frac{1}{\pi N_s(0)} \frac{\gamma_{q\nu}}{\omega_{q\nu}^2}, \quad (4)$$

where  $\gamma_{q\nu}$  is phonon linewidth,  $\omega_{q\nu}$  the dispersion relation of phonon,  $N_s(0)$  the electronic density (pre spin) at Fermi surface. The usual  $\lambda$  is the weighted average of  $\lambda_{q\nu}$  for different  $q$  points and the summation of all phonon bands or phonon modes. In this work, the  $\alpha^2 F(\omega)$ ,  $\gamma_{q\nu}$  and  $\lambda_{q\nu}$  are calculated using the linear response theory with the frame of the density functional theory based on the plane-wave pseudo-potential method [25]. We just simply use the  $q$ -independent Eliashberg function  $\alpha^2 F(\omega)$  in standard Eliashberg theory. A full treatment electron-phonon interaction needs  $q$ -dependent Eliashberg function  $\alpha^2 F(k, \omega)$  introduced in reference [26].

The ultra-soft pseudo-potential and the GGA approximation [27] are used in total-energy calculation of electronic structure [25]. In the calculations, two Monkhorst-Pack grids  $16 \times 16 \times 16$  and  $24 \times 24 \times 24$  are used for fcc and bcc structure, two grids of  $16 \times 16 \times 8$  and  $24 \times 24 \times 12$  for hcp structure. The Monkhorst-Pack grids for the phonon calculations are  $4 \times 4 \times 4$  and  $6 \times 6 \times 6$  for fcc and bcc,  $4 \times 4 \times 2$  and  $6 \times 6 \times 3$  for hcp structures respectively. The energy cutoffs are different for different elements within range from 400 eV to 550 eV.

Using the Eliashberg function  $\alpha^2 F(\omega)$  obtained from linear response theory and the standard strong-coupling theory, we can more reliably calculate  $T_c$  and other properties of superconductors. We have calculated the Eliashberg functions  $\alpha^2 F(\omega)$  of simple metals listing in Table.(1). We plot  $\alpha^2 F(\omega)$  functions of Ni, Pd and Pt in Fig.3(a), Cu, Ag and Au in Fig.3(b), Cd, La and Pb in Fig.3(c). From Table.(1), metallic Ni has relatively large hopfield parameter  $\langle \omega^2 \rangle \lambda$ , so it is a potential superconductor under extreme condition such as at high pressure similar to non-magnetic iron [9]. Our calculations have shown that the magnetic moment of Ni atom quenches to zero when pressure is higher than 300 GPa. The element Pd has smaller  $\lambda \sim 0.20$  and its superconductivity is only found in the samples after the irradiation with  $\text{He}^+$  [28]. The element Pt has relative larger  $\lambda$  value than the threshold  $\lambda_c$ , so it should be a superconductor. The superconductivity of element Pt, however, is only found in powder samples [29]. From Table.(1), the  $\lambda$  values of noble metals Cu, Ag and Au are all smaller than the threshold  $\lambda_c \sim 0.22 - 0.28$ , so the threshold effect for small  $\lambda$  in strong-coupling theory is indicative that noble metals Cu, Ag and Au have no superconductivity. It's correct even at high pressure (see next section). In Table.(1), the elements of heavy metals such as Pb, Hg, Cd and La have relative large  $\lambda$ . For metallic Pb, we use the norm-conservation pseudo-potential which gives better phonon spectrum and  $T_c$ . The Hg and Cd have smaller  $\langle \omega^2 \rangle \lambda$  values so these heavy metals have small space to increase  $T_c$  further at extreme condition such as high-pressure. The  $T_c$  in Table.(1) for Cd, Hg, Pb and La match the experimental values very well. These heavy metals have soft modes with imaginary energies at normal condition. This agrees with general arguments that the softening of vibration mode is intrinsic important to superconductivity. It's reasonable that we use the Coulomb pseudo-potential  $\mu^* \sim 0.1$  in strong coupling calculation for all simple metals under studied. This is because the obtained  $T_c$  are very close to experiments shown in Table.1. The



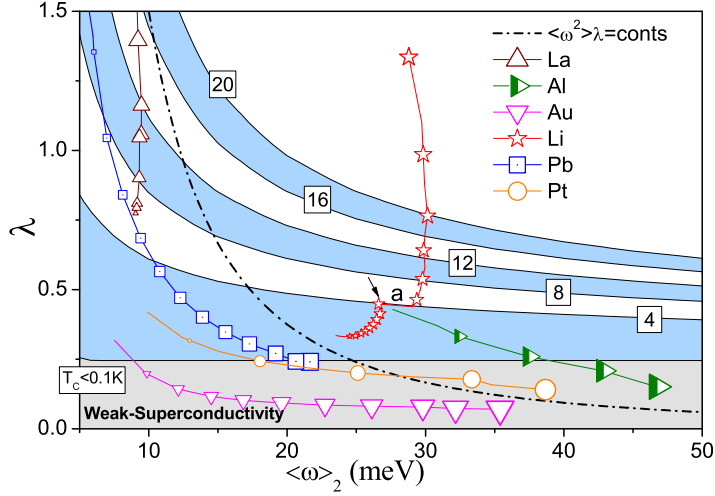


Figure 4: The evolutions of  $T_c$  with superconducting parameters  $\lambda$  and  $\langle\omega\rangle_2$  on  $T_c$  map for different metals with increasing pressure. The sizes of scatters in proportion to  $P^{1/5}$  measure the magnitude of pressure  $P$ . The arrow  $a$  points the break of curve for lithium at 13 GPa. The dash-dot line plot the curves  $\langle\omega^2\rangle\lambda=\text{cont.}$

underlying physical reason is probably that large band-width of these simple metals make the re-normalized  $\mu^*$  very close to 0.1.

## 5 The evolution of superconductivity with increasing pressure on $T_c$ map

As main purpose of this context, we study the evolutions of superconducting state on  $T_c$  map [3] when pressure increases. The static pressure is simply controlled by changing the cell volume. We plot the evolutions of superconducting parameters of Al, Au, Pt, Li, La and Pb on the map with increasing pressure shown in Fig.4. The  $\langle\omega\rangle_2$  is used to measure the phonon energy instead of  $\Omega_P$  used in previous papers [3]. The  $\lambda$  for Au decreases with pressure and  $\langle\omega\rangle_2$  increases with pressure, which is very similar to others noble metal Cu and Ag. The  $\lambda$  keeps smaller than  $\lambda_c$  is indicative that Au, Ag and Cu can not become superconductors within pressure ranges up to 300GPa. At ambient pressure, Pt is marginal superconductor, but its superconducting parameters enter non-superconductivity region when increasing pressure. The metal Al is real superconductor at ambient pressure and becomes non-superconductivity with increasing pressure. The metal Pb is a strong-coupling superconductor and  $T_c$  decreases with increasing pressure.

The positive  $dT_c/dP$  for La and Li with increasing the pressure are different from the negative  $dT_c/dP$  for Al, and Pb. For La and Li, the parameters of electron-phonon interaction  $\lambda$  increase with pressure and the  $\langle\omega\rangle_2$  changes relative small (even decrease). A structural instability happens at 13 GPa for

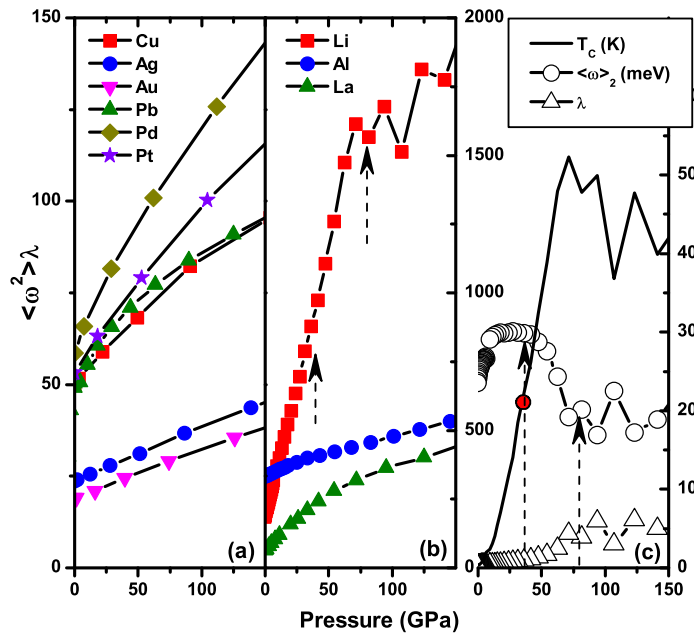


Figure 5: (a,b) The parameters  $\langle \omega^2 \rangle \lambda$  with unit  $(\text{meV})^2$  change with increasing pressure for different simple metals. (c)  $T_c$ ,  $\lambda$  and  $\langle \omega \rangle_2$  of metal Li change with increasing pressure. The two arrows in (b) and (c) respectively are corresponding to the structural phase-transitions of metal Li at pressures 40 GPa and 80 GPa.

Li. We recalculate the curve using norm-conserving pseudo-potential. The structural instability still remains however it becomes very weak. For Li, the ultra-soft pseudo-potential gives  $T_c=22\text{K}$  at pressure 36 GPa and for normal-conserving pseudo-potential  $T_c=20\text{K}$  at 15 GPa. Thus the results of ultra-soft pseudo-potential are more close to experimental  $T_c=20\text{K}$  at pressure 50 GPa in Ref. [4] and  $T_c=16\text{K}$  at 40 GPa in Ref [5]. Similar to Li, both  $\lambda$  and  $T_c$  of La increase with pressure and  $\langle\omega\rangle_2$  has only small change. The more sensitive response of  $\lambda$  than  $\langle\omega\rangle_2$  for applying pressure means that Li and La try to modify their lattice structures under high pressure. However for Pb, Pt, Au and Ag under high pressure the lattice structures are stable and the frequencies of phonons are more efficiently increasing with pressure.

An important relation  $\langle\omega^2\rangle\lambda=\text{constant}$  has been plotted on the  $T_c$  map. The relation had been used to explain the spatial anti-correlation between energy gap and phonon energy found in the samples of HTSC superconductor Bi2212 [3] and the anomalous isotope effects of  $\text{Rb}_3\text{C}_{60}$  [31]. A very useful formula of isotope effects had been derived [31] based on the relation. The pressure-dependent  $\langle\omega^2\rangle\lambda$  had been studied in detail using the formula of strong-coupling theory [32]. The Fig.5(a,b) show that  $\langle\omega^2\rangle\lambda$  does not keep as constant with increasing pressure. However our calculations show that the generalized relation  $M\langle\omega^2\rangle\lambda=\text{constant}$  is correct for isotope substitution for simple metals.

The curve  $\langle\omega^2\rangle\lambda$  of Pb is very close to the curves of Cu with non-superconductivity, Pt and Pd with weak superconductivity shown in Fig.5. The superconductivity of Pb is because of the large  $\lambda$  or strong-electron-phonon interaction. The atomic mass of Pt is very close to Pb but with very weak superconductivity. This is because the parameter  $\lambda$  of Pt is far less than that of Pb shown in Table.(1), although the phonon energy of Pt is almost twice higher than that of Pb shown in Fig.3. The parameter  $\langle\omega^2\rangle\lambda$  measures the possible maximum of  $T_c$ , however the individual values of  $\langle\omega^2\rangle$  and  $\lambda$  need to be considered to determine the real  $T_c$  of a superconducting material. The parameter  $\langle\omega^2\rangle\lambda$  increases with pressure for most of superconductors in Fig.5. However, this does not mean that  $T_c$  always increases with pressure. The depressed  $T_c$  with increasing  $\langle\omega^2\rangle\lambda$  such as for Pb ascribes to the decrease of  $\lambda$ . For metal Al the same situation is correct and its  $T_c$  decreases with increasing pressure and close to zero at 5 GPa [33], which is consistent with our calculations and others [34].

Experimentally, metal Li shows complex structural phase-transitions in diamond anvil when pressure increases up to 100 GPa. There are at least two phase transitions at around 40 GPa and around 70-80 GPa [13]. Around 20-40 GPa, fcc structure is stable.  $T_c$  reaches to 16K near 40GPa. From 40 GPa to 70-80 GPa the c/16 phase is stable and  $T_c$  keeps about 16K [5] (even reaches about 20K [4]). When pressure is higher than 80 GPa, a structural phase happens and  $T_c$  decreases. Compared with our results shown in Fig.5(b,c), the phonon energy  $\langle\omega\rangle_2$  significantly decreases at pressure around 40 GPa, and with pressure increasing further,  $\lambda$  reaches to the maximum at pressure around 80 GPa. Thus our results mean that, between 40 GPa to 80 GPa, the crystal structure is in an intermediate phase between two stable phases. At pressure 40 GPa, the fcc structure becomes unstable, the intermediate phase emerges from fcc phase by phonon softening. At pressure 70-80 GPa, the electron-phonon interaction reaches to the maximum. The intermediate phase becomes unstable and a new phase form by a phase transition. The big jump of resistivity of normal state (25K) at about 80 GPa just shows a real phase-transition [13]. The  $T_c$

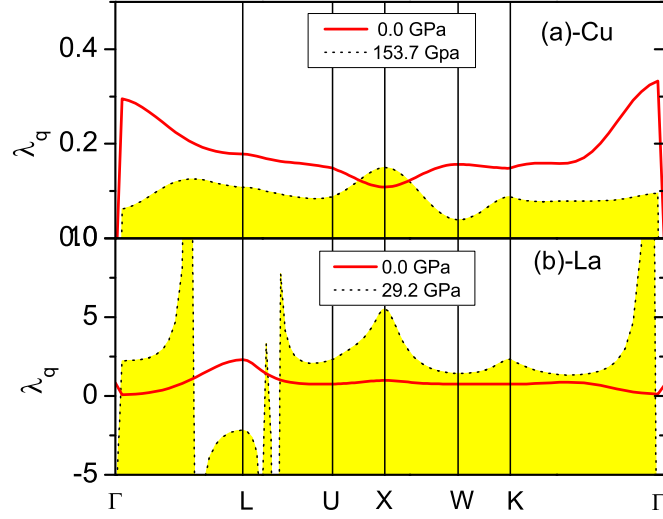


Figure 6: The  $q$ -dependent parameters  $\lambda_q$  of electron-phonon interaction at low pressure (solid line) and high pressure (dot-line) 153.7 GPa (Cu) and 29.2 GPa (La).

monotonously increases with pressure from 40 to 75 GPa in our calculations, which is different from keeping around 16K in experiment [5]. The discrepancy is probably because the stable structure is the  $c/16$  phase and not the fcc structure used in our calculation. When pressure increases to higher than 80 GPa,  $T_c$  decreases with pressure which is consistent with experiments. Although the fcc structure is kept unchanged from low to high pressure, our results still hint possible structural transitions of metal Li at corresponding experimental pressures. This means that the interactions of atomic orbits between nearest-nearby atoms plays more important role than the formation of super-structure of crystal with increasing pressure.

The pressure-dependent  $T_c$  of metal Li is very similar to superconducting niobium nitride (NbN). The observed high-pressure effect on  $T_c$  is explained as the pressure-induced interplay of electronic stiffness and phonon frequency [35]. In this paper, the high-pressure effect on Li is explained as the changes of role between electron-phonon interaction  $\lambda$  and phonon energy  $\langle\omega\rangle_2$  when pressure increase as illustrated in Fig.5(c). In low-pressure region, increasing  $T_c$  with pressure is induced by the increasing  $\lambda$ . In high-pressure ( $P > 80$  GPa) region, decreasing  $T_c$  with pressure is induced by softening of phonon modes.

## 6 The electron-phonon interaction of element metals under pressure

The superconductors collected on  $T_c$  map in Fig.4 can be divided into two groups: (1) metals La and Li; (2) metals Pb, Al and others. The effects of high pressure are more efficiently increasing  $\lambda$  for group (1) but increasing  $\Omega_P$  for

Fig.7 is missing

Figure 7: The Fermi surfaces of metal Cu at high pressure 153.7 GPa (a), and La (fcc) at low pressure 0.0 GPa (b) and high pressure 29.2 GPa (b).

group (2). As discussed in Ref.[14] based on experimental  $T_c$ -pressure relations, most of simple metals are belong to above two groups. We calculate  $q$ -dependent  $\lambda_q$  of La, Cu and other metals at different pressures. As a comparison, we present the results of non-superconductor Cu and superconductor La. The Cu is prefect conductor and the metal La with fcc structure is well-known superconductor at ambient pressure with  $T_c=6$  K [36]. At high pressure 20 GPa,  $T_c$  of La increases to 12.8K [36]. The electron-band, phonon-band and Eliashberg function  $\alpha^2F(\omega)$  of La had been studied in very details [20, 21].

The  $q$ -dependent parameters  $\lambda_q = \sum_{\nu} \lambda_{q\nu}$  of electron-phonon interaction generally have very large values near or at some high symmetry  $q$ -points shown in Fig.6. For metal Cu, the  $\lambda_{q\nu}$  decreases with increasing pressure but the  $\omega_{q\nu}$  increases with pressure. The one exception is that near K point,  $\lambda_q$  of Cu increases with pressure. The increase of  $\lambda_q$  at high symmetry point of Brillouin zone, such as K point of fcc crystal, means that the  $C_{2v}$  symmetry of the crystal will be possible broken if pressure increases further. The values of  $\lambda_q$  for metal La have maximum near high-symmetry points. Exactly at  $\Gamma$  point,  $\lambda_q$  is hard to define due to the large numerical errors. However, main features at others  $q$  points, especially the larger values of  $\lambda_q$  near  $\Gamma$  point along  $\Gamma - K$  line are very robust in Fig.6(b).

The phonon anomaly of fcc La at  $L$  point shown in Fig.6 were found in experiment of temperature-dependent phonon dispersion [37] and theoretical calculations [21]. The soft modes especially for transverse modes (shearing instability) lead to the instability of lattice. The distances (or interactions) between  $\langle 111 \rangle$  planes are larger (weaker) than those along other directions. The instability of lattice structure begins with transverse gliding between  $\langle 111 \rangle$  planes due to smaller activation energy.

We plot the Fermi surfaces of La at low pressure and at high pressure shown in Fig.7. At low pressure there is only one sheet of Fermi surface with rather

complex topology. The electrons occupy around the boundaries except that near the center region of eight hexagons and the 24 vertexes. When the pressure increases to 29.2 GPa, the topology of Fermi surface has significant changes. A group of very small Fermi-surface packets appear near the middle of  $\Gamma - K$  lines but they aren't displayed in Fig.7 due to very small sizes. The occupations of electrons near regions of eight hexagons have large reductions, especially near 36 edges. This means that the electronic states at the edges of Brillouin zone are electron-like states at low pressure and hole-like states at high pressure. The large reconstruction of Fermi surface for La will lead to the structural transition between different phases. For metal Cu, the increasing pressure only generates very small changes of lattice constant. So its electron-like Fermi surface has very small change at high pressure (153.7 GPa) shown in Fig.7 with the well-known shape of Fermi surface at ambient pressure.

The high-symmetry points of Brillouin zone characterize the long-range orders of crystal structure determined by space-group symmetries. The electrons with wave vectors near high symmetrical points, line and boundaries of Brillouin zone have potentially strong interactions with lattice vibrations. The main contributions to  $\lambda$  come from the parts of Fermi surface contacted with boundaries of Brillouin zone. This is why noble metals have very small  $\lambda$  and metal La, Pb and Hg have very larger  $\lambda$ . Thus, the structural phase transition will lead to the sharp increases of  $\lambda$  with increasing pressure for metal La.

## 7 conclusion

In summary, we have calculated  $T_c$  map in the region of weak electron-phonon coupling. The threshold effect of  $\lambda_c$  is found in small  $\lambda$  region. It originates from the competition between electron-phonon interaction and electron-electron Coulomb interaction when  $\lambda$  is comparable with  $\mu^*$ . The threshold effect of  $\lambda$  can explain why noble metals are not superconductors even at high pressure and why  $T_c$  of most of simple metals are higher than 0.1K. The phonon spectra and Eliashberg functions have been calculated by using linear response method in the framework of density functional theory. The obtained Eliashberg functions  $\alpha^2F(\omega)$  are then used in the calculations of strong-coupling theory. Our calculations illustrate how the superconducting parameters of simple metals distribute on the  $T_c$  map and how they run on the map with increasing pressure. Our results explain the pressure-dependent  $T_c$  of metal Li at high pressure ( $P > 80$  GPa). Thus the  $T_c$  maps studied in this paper and in previous papers [3] are very useful tools for studying the superconductivity of simple metals and hopefully extend to other types of superconductors.

## 8 Acknowledgements

The Fermi surfaces are plotted using XCrySden software. Zeng was supported by the special Funds for Major State Basic Research Project of China (973) under Grant 2007CB925004 and Zou by the National Science Foundation of China under Grant 10874186.

## References

- [1] P. B. Allen and R. C. Dynes, Phys. Rev. **B12** (1975), 905.
- [2] W. L. McMillan, Phys. Rev. **167** (1968), 331.
- [3] W. Fan, Physica C **469** (2009), 177; W. Fan, Chinese Physics Letter, **25** (2008), 2217.
- [4] K. Shimizu, H. Kimura, D. Takao, and K. Amaya, Nature (London) **419** (2002), 597.
- [5] V. V. Struzhkin, M. I. Eremets, W. Gan, H. K. Mao, R. J. Hemley, Science **298** (2002), 1213.
- [6] V. V. Struzhkin, R. J. Hemley, H. K. Mao and Y. A. Timofeev, Nature (London) **390** (1997), 382.
- [7] K. Shimizu, K. Suhara, M. Ikumo, M. I. Eremets, and K. Amaya, Nature (London) **393** (1998), 767.
- [8] E. A. Ekimov, V. A. Sidorov, E. D. Bauer, N. N. Mel'nik, N. J. Curro, J. D. Thompson, and S. M. Stishov, Nature (London) **428** (2004), 542.
- [9] K. Shimizu, T. Kimura, S. Furomoto, K. Takeda, K. Kontani, Y. Onuki, and K. Amaya, Nature (London) **412** (2001), 316.
- [10] T. Yabuuchi, T. Matsuoka, Y. Nakemoto, K. Shimizu, J. Phys. Soc. Japan **75** (2006), 083703.
- [11] J. J. Hamlin, V. G. Tissen, and J. S. Schilling, Phys. Rev. **B 73** (2006), 094522.
- [12] Y. M. Ma, M. Eremets, A. R. Oganov, Y. Xie, I. Trojan, S. Medvedev, A. O. Lyakhov, M. Valle, and V. Prakapenka, Nature (London) **458** (2009), 182.
- [13] T. Matsuoka, and K. Shimizu, Nature (London) **458** (2009), 186.
- [14] C. Buzea, and K. Robbie, Supercond. Sci. Technol. **18** (2005), R1-R8.
- [15] S. Y. Savrasov, D. Y. Savrasov, Phys. Rev. **B 54** (1996), 16487.
- [16] S. K. Bose, J. Phys.: Condens. Matter **21** (2009), 025602.
- [17] D. Kasinathan, J. Kuneš, A. Lazicki, H. Rosner, C. S. Yoo, R. T. Scalettar, and W. E. Pickett, Phys. Rev. Lett. **96** (2006), 047004.
- [18] N. E. Christensen, and D. L. Novikov, Phys. Rev. **B 73** (2006), 224508.
- [19] Z. P. Yin, S. Y. Savrasov, and W. E. Pickett, Phys. Rev. **B 74** (2006), 094519.
- [20] W. E. Pickett, A. J. Freeman, and D. D. Koelling, Phys. Rev. **B 22** (1980), 2695.

- [21] H. M. Tütüncü, and G. P. Srivastava, *Journal of Applied Physics* **104** (2008), 063916.
- [22] H. S. Wu, J. H. Cai, C. D. Gong, G. D. Ji, J. D. Cai, *Acta Physica Sinica* **26** (1977), 509. (in Chinese)
- [23] C. D. Gong, H. S. Wu, J. H. Cai, J. D. Cai, and G. D. Ji, *Acta Physica Sinica* **27** (1978), 85. (in Chinese)
- [24] H. S. Wu, Z. Y. Weng, G. D. Ji, Z. F. Zhou, *J. Phys. Chem. Solids* **48** (1987), 395.
- [25] QUANTUM-ESPRESSO is a community project for high-quality quantum-simulation software, based on density-functional theory, and coordinated by Paolo Giannozzi. See <http://www.quantum-espresso.org> and <http://www.pwscf.org>.
- [26] P. B. Allen and B. Mitrovic, in *Solid State Physics* **Vol 37**, (1982) 1, edited by F. Seitz and D. Turnbull (Academic, New York).
- [27] J. P. Perdew, K. Burke and M. Ernzerhof, *Phys. Rev. Lett.* **77** (1996), 3865.
- [28] B. Stritzker, *Phys. Rev. Lett.* **41** (1979), 1769.
- [29] A. Schindler, R. König, T. Herrmannsdörfer, H. F. Braun, G. Eska, D. Günther, M. Meissner, M. Mertig, R. Wahl, W. Pompe, *Physica B* **329-333** (2003), 1427.
- [30] R. Bauer, A. Schmid, P. Pavone, D. Strauch, *Phys. Rev. B* **57** (1997) , 11276.
- [31] W. Fan, to appear in *International Journal of Modern Physics B*; preprint 2008, arXiv:0811.3813.
- [32] X. J. Chen, H. Zhang, and H. -U. Habermeier, *Phys. Rev. B* **65** (2002), 144514.
- [33] D. U. Gubser, and A. W. Webb, *Phys. Rev. Lett.* **35** (1975), 104.
- [34] G. Profeta, C. Franchini, N. N. Lathiotakis, A. Floris, A. Sanna, M. A. L. Marques, M. Lüders, S. Massidda, E. K. U. Gross, and A. Continenza, *Phys. Rev. Lett.* **96** (2006), 047003.
- [35] X. J. Chen, V. V. Struzhkin, Z. G. Zhu, R. E. Cohen, S. Kung, H. K. Mao, R. J. Hemley, and A. N. Christensen, *Phys. Rev. B* **72** (2005), 094514.
- [36] M. B. Maple, J. Wittig, and K. S. Kim, *Phys. Rev. Lett.* **23** (1969), 1375.
- [37] C. Stassis, C. -K. Loong, and J. Zarestky, *Phys. Rev. B* **26** (1982), 5426.